STM JOURNALS

Journal of
Polymer & Composites

ISSN: 2321-2810 (Online)
ISSN: 2321-8525 (Print)
Volume 14, Issue 2, 2026
DOI (Journal): 10.37591/JoPC

https://journals.stmjournals.com/jopc

Research JoPC

Fluid Dynamics of a Stressed Freshwater Lens: Integrated Flow Modeling and Pathways for Material-Centric Interventions in Khadir Island, Gujarat

Sagar Vinodray Nimavat[1], Mahendrasinh Shivraj Gadhavi[2,*]

Abstract

This study applies principles of fluid dynamics and porous media mechanics to analyze the behavior and sustainability of the freshwater lens in Khadir Island, an arid sedimentary island in Gujarat, India. We develop an integrated fluid flow model that couples surface hydrology with aquifer dynamics to quantify recharge fluxes, extraction stresses, and hydraulic responses. Using 11-year hydro-meteorological data (2011–2021) and sectoral demand projections, we characterize the island's water budget through a mass conservation framework. Results show total demand of 1,318.42 MLY, with agricultural extraction dominating the flux regime. Despite apparent annual surpluses, the system exhibits severe hydraulic stress, evidenced by a Water Exploitation Index of 72.1%, summer hydraulic head declines averaging 2.8 m, and a thinning freshwater lens (15–25 m). Flow analysis reveals critical temporal mismatches: monsoon recharge peaks are misaligned with dry-season demand peaks, creating a June deficit of 102.2 ML. Beyond diagnosis, the study transitions to a solution-oriented framework, arguing that the identified hydraulic inefficiencies represent classic problems of material performance [19]. We propose that the path to sustainability lies in engineered material interventions, specifically the development and deployment of advanced polymer and composite systems for seepage control [20], managed recharge [21], and monitoring [28]. This work thus provides a physically-based diagnostic methodology and lays a clear engineering blueprint for material scientists to develop targeted solutions for water security in data-scarce arid islands.

Keywords: Composite systems in hydrology, fluid transport modeling, materials for seepage control, polymer-based water retention, porous media flow, sustainable resource engineering

***Author for Correspondence**
Mahendrasinh Shivraj Gadhavi
E-mail id: mahendrasinh@gmail.com

[1]Research Scholar, Civil Engineering, Gujarat Technological University, Ahmedabad, Gujarat, India
[1]Lecturer, Civil Engineering Department Dr. S. & S. S. Ghandhy College of Engineering and Technology, Surat, Gujarat, India
[2]Assistant Professor, Civil Engineering Department L.D. College of Engineering, Ahmedabad, Gujarat, India

Received Date: January 28, 2026
Accepted Date: February 17, 2026
Published Date: March 12, 2026

Citation: Sagar Vinodray Nimavat, Mahendrasinh Shivraj Gadhavi. Fluid Dynamics of a Stressed Freshwater Lens: Integrated Flow Modeling and Pathways for Material-Centric Interventions in Khadir Island, Gujarat. Journal of Polymer & Composites. 2026; 14 (2): 12–29p.

INTRODUCTION

Small islands in arid regions represent critical case studies in confined fluid dynamics, where limited freshwater storage, saline intrusion risks [7], and climate variability [43] challenge the stability of fragile aquifer systems [1]. Khadir Island, located in the hyper-arid Kutch basin of Gujarat, India, is a sedimentary island whose freshwater lens dynamics are governed by complex lithology, episodic recharge, and growing anthropogenic extraction. The island supports approximately 17,257 residents and significant agricultural activity despite receiving erratic rainfall averaging 419.8 mm annually. The presence of the UNESCO World Heritage site of Dholavira adds tourism-induced water demand, making sustainable fluid management a pressing concern [2].

Previous fluid dynamics research on island aquifers has emphasized the Ghyben-Herzberg relationship and the vulnerability of freshwater lenses to pumping-induced saline intrusion [3, 4]. However, most studies focus on oceanic atolls or temperate islands, with limited attention to arid sedimentary islands with complex lithological heterogeneity [2]. In such settings, the conventional assumption of homogeneous aquifer properties fails, and compartmentalized flow becomes significant [5]. Furthermore, integrated assessments that couple surface runoff models with subsurface flow dynamics to project sectoral demand are rare in island hydrology literature. Critically, while hydrological diagnostics are well-developed, there remains a significant gap in translating these quantitative findings into specifications for next-generation engineering materials that can systemically alter water budgets [25].

This study addresses these gaps through a three-phase approach: (i) to develop an integrated fluid flow model that quantifies the aquifer's hydraulic status and inefficiencies; (ii) to assess freshwater lens stability through a mechanistic water budget; and (iii) to reframe the identified hydrological challenges—specifically seepage losses, inefficient recharge, and data scarcity—as explicit performance requirements for novel polymer and composite materials [26], thereby bridging fluid dynamics with materials engineering for sustainable solutions.

METHODS

Fluid Dynamics and Solution-Scoping Framework

The study employs a multi-module, iterative framework designed to progress from systemic diagnosis to the specification of engineering solutions. This framework integrates: (1) surface water flux estimation using rainfall-runoff modeling, (2) subsurface recharge and flow modeling using porous media equations validated with field data, (3) granular, sectoral extraction quantification down to the village level, and (4) a coupled, time-variable water budget and lens stability analysis. Critically, a fifth, interpretive phase was embedded within the analytical process. This phase involved translating quantified hydrological inefficiencies—like the seepage loss rate of 40% or the 102.2 ML summer deficit—into explicit, quantifiable performance parameters for potential material interventions.

The relationship between hydrological diagnostics and corresponding material performance targets is summarized in Table 1. To ensure a transparent and quantitative bridge between hydrological diagnosis and materials engineering design, the following translation protocol was applied to all major model outputs:

Table 1. Integrated fluid dynamics and solution-scoping framework.

S no	Model output (hydrological diagnosis)	Derived material performance target	Relevant material class
1	40% conveyance loss in earth canals (Section 3.2.2)	Hydraulic conductivity of lining material < 1×10^{-8} m/s	Polymer-modified composite liners, geosynthetic clay liners (GCLs) [19, 20]
2	Critical June deficit of 102.2 ML (Section 3.2.3)	Water retention capacity: 100–150 ML over 90-day dry period	Superabsorbent polymer (SAP) hydrogels, biopolymer composites [21, 24]
3	TDS > 4000 mg/L in eastern villages (Section 3.1.3)	Corrosion resistance: stable in saline environments (TDS > 4000 mg/L, Cl^- > 2000 mg/L) for >5 years	Fiber-reinforced polymer (FRP) composites, epoxy-based encapsulants [28, 33]
4	Pre-monsoon water level decline of 2.8 m (Section 3.3.2)	Recharge enhancement: minimum 20% increase in infiltration rate	Porous polymer aggregates, hydrogel-amended soils [22, 38]
5	Spatial extraction flux disparity (3.06–29.98 m^3/day/km^2) (Section 3.3.1)	Targeted deployment: materials configurable for point-of-need application	Modular composite systems with variable permeability [25, 26]

Data Collection and Pre-Processing

Hydro-meteorological Data

Daily gridded rainfall data (0.25° x 0.25° resolution) for the period 2011–2020 were obtained from the India Meteorological Department (IMD). To ensure accuracy for the local scale, these data were cross-validated against manual rain gauge records maintained at the Dholavira heritage site for the overlapping period (2015–2020), applying a linear correction factor where minor systematic biases were observed. Missing daily values (<2% of the record) were infilled using spatial interpolation from the three nearest grid points. Daily reference evapotranspiration (ET_0) was calculated using the FAO Penman-Monteith method [15], utilizing gridded meteorological data (maximum and minimum temperature, relative humidity, wind speed, solar radiation) from the same IMD source. Wind speed data, measured at 2m height, were converted to the standard 10m height using a logarithmic wind profile correction before use in the ET_0 calculation.

Hydrogeological Field Monitoring

A network of 15 existing groundwater monitoring wells, managed by the Gujarat Water Resources Department and spread across the nine villages, formed the core of the subsurface data collection. Well locations were geotagged using a handheld GPS unit (Garmin GPSMAP 64s) with an average horizontal accuracy of ±3 meters. The elevation of the measuring point (MP) for each well was established by differential leveling to a common benchmark, creating a consistent vertical datum across the island. Seasonal water level measurements (pre-monsoon in May, post-monsoon in October) were conducted manually using an electric water level indicator (Solinst 101) with a precision of ±1 cm. For six key wells with long-term records (including HPII_KCH_006 and KC-13), all historical data (1992–2019) were digitized from paper logs, cross-checked for transcription errors, and compiled into a unified temporal database, allowing for trend analysis over nearly three decades.

Hadrochemical Sampling and Analysis

Groundwater samples were collected from the monitoring network during the pre- and post-monsoon campaigns of 2021. Prior to sampling, each well was purged by extracting at least three well-casing volumes to ensure the collection of fresh aquifer water. Samples were filtered in the field through 0.45 µm cellulose acetate membranes. On-site measurements of pH, Electrical Conductivity (EC), and temperature were taken using a calibrated multi-parameter probe (Hanna HI98194). Samples for cation analysis were acidified with ultrapure nitric acid to pH <2. All samples were stored in pre-cleaned HDPE bottles on ice and transported to the laboratory within 24 hours. Major ions (Ca^{2+}, Mg^{2+}, Na^{+}, K^{+}, Cl^{-}, SO_4^{2-}, HCO_3^{-}, CO_3^{2-}) were analyzed following standard APHA methods. Calcium and magnesium were determined by EDTA titration, sodium, and potassium by flame photometry (Systemics Flame Photometer 128), chloride by argentometric titration, sulfate by turbidimetry, and carbonate/bicarbonate by acid titration. Charge balance errors for all analyzed samples were within the acceptable limit of ±5%.

Geotechnical and Soil Characterization

Undisturbed soil cores were extracted from three strategically located boreholes (drilled to 75m depth for a separate geotechnical survey) using a thin-walled Shelby tube sampler. Core samples were taken at intervals of 0–12m, 13–37m, and 38–75m to characterize vertical heterogeneity. Particle size distribution was determined using the hydrometer method (ASTM D7928) after removing organic matter with hydrogen peroxide and dispersing with sodium hexametaphosphate. Soil textural class was determined using the USDA soil texture triangle. Bulk density (ρ_b) was measured on intact core segments using the core method, and particle density (ρ_s) was measured with a water pycnometer. Total porosity (n) was then calculated as $n = 1 - (\rho_b / \rho_s)$. Effective porosity (n_e) was estimated as 0.75n, based on typical values for sandy clay loam textures.

Socio-Economic and Sectoral Demand Data

Primary census data for 2011 at the village level was obtained from the Census of India portal. The 2021 projected population was calculated by applying a compounded annual growth rate (CAGR) of

1.5%, derived from the observed growth trend in Kutch district between the 2001 and 2011 censuses. This projection was validated through discussions with local panchayat officials, who confirmed stable population trends without significant in- or out-migration. Livestock census data (number of cattle, buffalo, sheep, goats) for each village for the year 2020 was acquired from the District Animal Husbandry Department. Cropping patterns, sown area (ha) for the Kharif (Bajra, Jeera), Rabi (vegetables, fodder), and Summer (vegetables) seasons, and average yield data for the 2020–21 agricultural year were compiled from reports of the local Agriculture Department office. Where official records were incomplete, data was supplemented through structured interviews with 15 farmers across the major villages to ensure representativeness.

Analytical Methods

Surface Runoff Modeling

The Soil Conservation Service Curve Number (SCS-CN) method [10, 11] was employed to estimate direct surface runoff (Q) from rainfall (P). The method is expressed as:

$Q = (P - I_a)^2 / (P - I_a + S)$ for $P > I_a$,

where I_a is the initial abstraction and S is the potential maximum retention.

We adopted the standard assumption that $I_a = 0.2S$. Thus, the equation simplifies to the form used in our model:

$Q = (P - 0.2S)^2 / (P + 0.8S)$.

The retention parameter S (in mm) is related to the Curve Number (CN) by: $S = (25400 / CN) - 254$.

The Curve Number (CN) is a dimensionless parameter representing runoff potential, integrating soil type, land use, and antecedent moisture conditions (AMC). Based on our land use/land cover classification and the hydrological soil group (HSG) of the island's soils (Group C: slow infiltration), a composite, area-weighted average CN of 75 was derived for AMC-II (average moisture conditions). This value is consistent with established ranges for arid rangelands and agricultural areas [10, 11]. Runoff was calculated on a daily time step and aggregated annually.

Groundwater Recharge Estimation

Natural groundwater recharge (R) was estimated primarily using the Water Table Fluctuation (WTF) method [13], which is well-suited for unconfined aquifers with pronounced water level rises in response to recharge events. The method is expressed as:

$R = S_y \Delta h A$

Where S_y is the specific yield (dimensionless), Δh is the rise in the water table (m) over the recharge period (here, from pre-monsoon to post-monsoon), and A is the area (m^2) over which the rise is averaged.

Specific yield (S_y) is the most critical and uncertain parameter. We used a value of 0.12, derived from published values for the clayey sand lithology that dominates the island [12]. To assess uncertainty, a sensitivity analysis was conducted using a plausible range of S_y from 0.08 to 0.16. The rise in water table (Δh) was calculated as the difference between the spatially averaged post-monsoon (October) and pre-monsoon (May) water levels across the 15-well network for each year. The recharge area (A) was taken as the entire island area (315.20 km^2) minus areas classified as exposed rock or deep saline water, approximated as 90% of the total area (283.68 km^2).

Aquifer Properties, Freshwater Lens Delineation, and Saltwater Interaction Dynamics

The classic Ghyben-Herzberg approximation [3, 4] was used to provide a first-order estimate of the freshwater lens thickness (h_f) beneath the water Table:

$h_f = (\rho_s / (\rho_s - \rho_f)) \times h$

Where ρ_s is the density of saline groundwater (assumed 1025 kg/m³), ρ_f is the density of fresh groundwater (1000 kg/m³), and h is the height of the freshwater head above sea level (m). This simplifies to $h_f \approx 40h$, indicating that for every meter the freshwater head is above sea level, the freshwater lens extends approximately 40 meters below it. The freshwater head (h) at any point was calculated by subtracting the measured water level (below ground level) from the ground surface elevation (obtained from a 30m resolution SRTM DEM) and then referencing it to mean sea level.

Transient Saline Intrusion and Interface Dynamics

While the Ghyben-Herzberg principle provides a useful static estimate of lens thickness, it assumes hydrostatic equilibrium and does not capture the dynamic behavior of the saltwater-freshwater interface under pumping stress [7]. To assess the transient response of the interface to anthropogenic abstraction, we applied a simplified analytical solution based on the method of Strack [1976] for steady flow in coastal aquifers:

$$\zeta(x) = \sqrt{[\ (2q\ x) / (K(1+\delta)) + (\zeta_0)^2\ ]}$$

Where $\zeta(x)$ is the depth to the interface at distance x from the coastline, q is the fresh groundwater flux per unit coastline, K is hydraulic conductivity, $\delta = (\rho_s - \rho_f)/\rho_f$, and ζ_0 is the interface depth at the coastline. This formulation allows estimation of how increased pumping (which reduces q) causes the interface to migrate inland.

For localized pumping wells, the risk of saline upconing was evaluated using the critical rise criterion of Dagan and Bear [7]:

$$z_{crit} = 0.5 \times (Q / (\pi\ K\ (1+\delta)\ i))$$

Where z_{crit} is the critical rise of the interface before well intrusion, Q is the pumping rate, and i is the ambient hydraulic gradient. Wells with screen intervals within z_{crit} of the estimated interface were flagged as high-risk for upcoming.

Seasonal Interface Fluctuation

To capture the seasonal dynamics of the saltwater interface, we applied a simplified transient correction based on the water table fluctuation method. The seasonal displacement of the interface ($\Delta\zeta$) was estimated from:

$$\Delta\zeta = (\rho_f / (\rho_s - \rho_f)) \times \Delta h \times S_y$$

Where Δh is the seasonal water table fluctuation (pre-monsoon to post-monsoon) and S_y is specific yield. This relationship, derived from the Ghyben-Herzberg principle and mass conservation, indicates that a 1 m rise in water table during monsoon corresponds to approximately 40 m of downward displacement of the interface—a rapid response that highlights the dynamic nature of the system. Conversely, the 2.8 m average pre-monsoon water level decline documented in Section 3.3.2 implies an upward migration of the interface by approximately 112 m during the dry season, bringing saline water closer to pumping zones.

Limitations and Future Modeling Needs

It is important to acknowledge that the analytical methods described above provide first-order estimates suitable for diagnostic assessment and material intervention scoping. Precise mapping of the time-variant saltwater-freshwater interface under heterogeneous aquifer conditions and transient pumping stresses would require a density-dependent, numerical flow and transport model (, e.g., SEAWAT or FEFLOW). Such high-resolution modeling is recommended as a future research priority following the initial material intervention trials proposed in Section 4.3. However, for the purposes of defining material performance requirements—specifically the corrosion resistance thresholds (Section 2.1.1) and the spatial prioritization of intervention zones (Table 4)—the current analytical framework provides sufficient quantitative guidance.

Groundwater Flow and Solute Transport Potential

Horizontal groundwater flow velocity (v) was estimated using Darcy's Law for flow in porous media [5]:

v = (K * i) / n_e

Where K is the hydraulic conductivity (m/day), i is the hydraulic gradient (dimensionless), and n_e is the effective porosity.

Hydraulic conductivity (K) was estimated from grain-size analysis of the soil samples using the empirical Hazen formula: K (cm/s) = C * $(d_{10})^2$, where C is a coefficient (typically 100 for clean sands) and d_{10} is the effective grain size (cm) at which 10% of the sample is finer. The calculated K values ranged from 0.5 to 2.3 m/day. The hydraulic gradient (i) was calculated by constructing a water table contour map for the pre-monsoon period using kriging interpolation of the well data in QGIS and measuring the slope along the inferred dominant flow direction. The average linear velocity (v) was then used in a simplified advection-dispersion model to estimate the minimum time for a conservative solute (like chloride) to travel from the island's saline boundaries to interior extraction zones.

Sectoral Water Demand Calculation

Demand was calculated on a daily basis and then aggregated annually (MLY) for consistency with recharge estimates. All calculations were performed at the village level and summed for the island total.

- *Domestic Demand:* Q_domestic = Σ (P_i *135 LPCD), where P_i is the projected 2021 population of village* i* and 135 LPCD is the design standard for rural water supply in Gujarat [GWSSB, 2021].
- *Agricultural Demand*: This was the most complex calculation. Crop water requirement (CWR_k in cm) for each crop (k) was estimated using the FAO-56 single crop coefficient approach [15]: CWR_k = ET_0 K_c_k, where K_c is the crop coefficient for each growth stage. The cropping calendar (sowing and harvest dates) was established from farmer interviews. The net irrigation requirement (NIR) was then CWR_k minus effective rainfall. As flood irrigation is predominant, a low application efficiency (η) of 0.60 was used to convert NIR to gross irrigation demand: Q_agri_k = (NIR_k A_k 10,000) / (100 η). The factor 10,000 converts hectares to m², and 100 converts cm to m.
- *Livestock Demand:* Q_livestock = Σ (N_j *WR_j),* where N_j is the number of animals of type j* (cattle, buffalo, sheep, goat) and WR_j is the daily water requirement per animal from ICAR standards [14].
- *Tourism Demand:* Q_tourism = (T_avg *D* 150 LPCD), where T_avg is the average daily tourist count (500), D is the estimated number of tourist days per year (300), and 150 LPCD is a standard estimate for tourist water use in arid regions.

Water Budget and Sustainability Indices

A monthly water budget was constructed for a representative year using average data:

ΔS = (P - ET - Q_surf) + (R) - (Q_domestic + Q_agri + Q_livestock + Q_tourism)

Where ΔS is the change in aquifer storage, P is precipitation, ET is actual evapotranspiration (scaled from ET_0 using crop coefficients and vegetated area), Q_surf is surface runoff, and R is recharge. A positive ΔS indicates storage gain, while negative indicates depletion.

The Water Exploitation Index (WEI) [16] was calculated annually as:

WEI = (Total Annual Abstraction / Total Annual Renewable Resources) * 100%

Renewable Resources were defined as the sum of average annual recharge and utilisable surface runoff. A WEI > 20% indicates water stress, >40% indicates severe stress, and >100% indicates over-exploitation of renewable resources.

Geospatial and Statistical Analysis

All spatial data (well locations, land use, soil types) were managed and analyzed in a Geographic Information System (QGIS 3.22). Interpolation of water levels was performed using ordinary kriging. Statistical analyses, including descriptive statistics, trend analysis using the Mann-Kendall test for water level time series, and linear regression for rainfall-runoff relationships, were conducted using R software (version 4.2.1). All plots and graphs were generated using the ggplot2 package in R.

Scenario and Sensitivity Analysis

To explore future sustainability pathways, three scenarios for the year 2030 were developed:

1. Business-As-Usual (BAU): Assumes a 2% annual compounded growth in all sectoral demands (based on recent trends) and no change in irrigation efficiency or recharge.
2. Improved Efficiency (IE) Scenario: Assumes widespread adoption of water-saving measures. This includes a shift from flood irrigation (η=0.60) to drip irrigation (η=0.85) for 80% of the cropped area [41], coupled with a 10% reduction in domestic water use through awareness and leakage repair programs.
3. *Managed Aquifer Recharge (MAR) Scenario*: Assumes the construction of 50 decentralized recharge structures (, e.g., percolation tanks, recharge wells) in high-infiltration zones, leading to a 20% increase in the effective annual recharge captured and stored [37, 39].

Sensitivity analysis was performed on the key model parameters. The WEI was recalculated by independently varying annual recharge (±20%) and total demand (±10%) to identify which parameter had the greatest influence on the stress indicator, expressed as the elasticity: (Δ%WEI / Δ%Parameter).

RESULTS

Comprehensive System Characterization

Hydro-Meteorological Patterns

Analysis of the 2011–2020 rainfall record revealed the high inter-annual variability characteristic of arid climates. Annual rainfall ranged from 103 mm (2018) to 932 mm (2011), with a mean of 419.8 mm and a standard deviation of 256.1 mm (coefficient of variation = 61%). This high variability underscores the inherent unreliability of the primary water source. A Mann-Kendall trend test on the annual series indicated no statistically significant trend ($p > 0.1$) over the decade. However, the distribution was sharply seasonal: an average of 89% (range: 85–94%) of the annual total fell within the core monsoon months of June to September. The mean annual reference evapotranspiration (ET_0) was calculated to be 2140 mm, approximately five times the average rainfall, creating a permanent, large atmospheric water demand.

Aquifer Hydraulic Properties and Freshwater Lens

Analysis of the 75m soil core revealed three distinct hydrostratigraphic units:

- *Unit 1 (0–12m)*: A mixture of clayey sand and shale fragments, with an average sand content of 83.4% (±5.4). The calculated hydraulic conductivity (K) using the Hazen formula was 1.8 m/day (±0.7). This unit acts as the primary unconfined aquifer.
- *Unit 2 (13–37m):* A more clay-rich zone with sand content decreasing to 76.9% (±6.1), indicating lower permeability (K ~ 0.9 m/day).
- *Unit 3 (38–75m):* Dominated by weathered shale and sandstone with sand at 73.3% (±7.2), likely representing a semi-confined to confined system with poor yield.

The estimated freshwater lens thickness, using the Ghyben-Herzberg principle and an average pre-monsoon freshwater head of 0.6m above sea level, ranged from 15 to 25 meters across the island. This thin lens is the sole sustainable freshwater resource and is highly vulnerable to over-pumping and saline intrusion. This thin lens thickness is consistent with observations from other arid islands where limited recharge and high evapotranspiration constrain freshwater storage [6]

Hydrochemical Facies and Salinization

Piper diagram analysis of the 2021 water quality data revealed two dominant hydrochemical facies: 1) Mixed Ca-Na-HCO_3 type in the western and central villages (Janan, Ratanpar), indicative of recharge areas with shorter residence time; and 2) Na-Cl type in the eastern villages (Kalyanpur, Gadhada), which is characteristic of saline intrusion and/or evaporative concentration. Chloride concentrations showed a clear spatial pattern, increasing from west (<1200 mg/L) to east (>4000 mg/L). A strong linear relationship ($R^2 = 0.91$) was observed between chloride (Cl^-) and Total Dissolved Solids (TDS), confirming that salinity is primarily driven by the influx of ancient saline water from the surrounding Rann, rather than evaporative enrichment of inland salts. This is a critical finding, as it points to a physical displacement process (saline intrusion) that is more challenging to reverse than concentration via evaporation. The seasonal variation in groundwater quality indicators and inferred recharge efficiency across villages is summarized in Table 2.

Table 2. Pre- and post-monsoon groundwater quality indicators (TDS, Cl^-) for selected villages in Khadir Island (2015–2020 average). The post-monsoon dilution provides an indicator of active recharge efficiency, which guides the siting of material-based managed aquifer recharge (MAR) interventions.

S no	Village	Pre-monsoon TDS (mg/L)	Post-monsoon TDS (mg/L)	% Reduction in TDS	Pre-Monsoon Cl^- (mg/L)	Post-monsoon Cl^- (mg/L)	Inferred recharge efficiency & salinity risk	Priority for MAR with composites
1	Ratanpar	2,450	1,820	-25.70%	~1,250	~938	Very High. Strong dilution indicates excellent recharge potential and active flushing. Low salinity risk.	Highest Priority. Ideal for piloting hydrogel-composite recharge structures.
2	Janan	1,490	1,110	-25.50%	~900	~675	Very High. Similar to Ratanpar. High-quality recharge zone with good freshwater flux.	Highest Priority. Prime location for composite-based MAR.
3	Kalyanpar	2,240	1,940	-13.40%	4,112	3,580	Moderate-Low. Some recharge occurs but is insufficient to significantly flush high background salinity. High intrusion risk [7].	Medium. Req uires composites that also act as semi-permeable barriers to impede saline advance.
4	Dholavira	2,150	1,900	-11.60%	~1,860	~1,674	Moderate. Moder ate recharge but starting from moderate salinity. Tourism pressure increases demand.	Medium. Focu s on demand-side composites (linings) and targeted MAR.
5	Amrapar	2,185	1,905	-12.80%	~1,900	~1,710	Moderate. Compa rable to Dholavira. Balanced recharge and salinity challenge.	Medium.

Hydrochemical data identifies western villages (Ratanpar, Janan) as high-efficiency recharge zones (>25% TDS reduction), ideal for managed aquifer recharge composites, while eastern sites show high salinity from intrusion, demanding materials with superior corrosion resistance.

Detailed Water Budget and Demand Analysis

Sectoral Demand Breakdown (2021)

The total annual water demand for Khadir Island in 2021 was quantified at 1,318.42 Million Liters per Year (MLY), equivalent to 3.61 MLD. The sectoral distribution was dominated by agriculture, which accounted for 1,097.45 MLY (83.3% of the total). Within agriculture, Bajra alone consumed 755.2 MLY, representing 57.3% of the island's total demand and 68.8% of agricultural demand. Domestic use was the second-largest sector at 148.15 MLY (11.2%), followed by livestock at 64.3 MLY (4.9%) and tourism at 8.52 MLY (0.6%). The per capita domestic water use of 135 LPCD, while a design standard, may represent an overestimate of actual use; however, it provides a consistent benchmark for planning.

Supply and the Water Exploitation Index

The average annual renewable freshwater resource, calculated as recharge plus utilisable runoff for the 2011–2020 period, was 956.67 MLY. Comparing this to the 2021 demand of 1,318.42 MLY yields a Water Exploitation Index (WEI) of 137.8% for that specific year. The average WEI over the decade, using average annual resources (956.67 MLY) against the linearly interpolated demand for each year, was 72.1%. Both figures are alarming. The annual figure >100% indicates that in 2021, abstraction exceeded the entire renewable supply, necessitating "mining" of fossil groundwater or storage. The decadal average >40% confirms a state of severe and chronic water stress [16]. The sensitivity analysis showed that the WEI has an elasticity of -0.65 with respect to recharge (a 10% increase in recharge leads to a 6.5% decrease in WEI) and +0.35 with respect to demand. This quantifies that enhancing recharge is a more powerful lever for reducing stress than marginally curbing demand. The detailed annual water balance components and calculated Water Exploitation Index (WEI) for the study period are presented in Table 3. The temporal evolution of water availability, demand, and WEI from 2011–2020 is illustrated in Figure 1.

Inter-annual data reveals a fundamental mismatch: while renewable water resources are highly variable (avg. ~665 ML), demand is consistently high (~1,257 ML), resulting in a decadal average WEI of 72.1% and confirming chronic, unsustainable groundwater mining that necessitates engineered interventions.

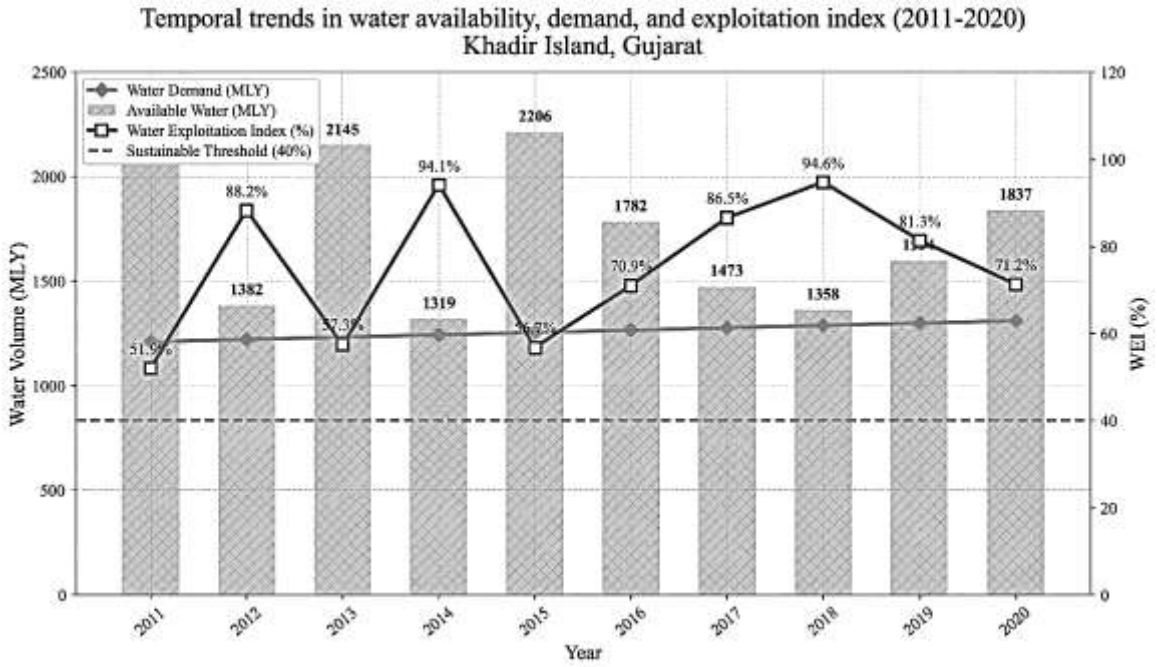

Figure 1. Temporal trends in water exploitation index (WEI), availability, and demand (2011–2020).

Table 3. Annual water balance components, total demand, and calculated water exploitation index (WEI) for khadir island (2011–2020). renewable resources are the sum of groundwater recharge and utilizable surface runoff. A WEI > 40% indicates severe water stress [16].

S no	Year	Rainfall (mm)	Groundwater recharge (ML)	Utilizable runoff (ML)	Total renewable resources (ML)	Total demand (ML)	Water exploitation index (WEI) (%)	Annual storage change (ΔS, ML)
1	2011	932	1,099.80	155.8	1,255.60	1,207.50	96.2	48.1
2	2012	255	471.5	36.2	507.7	1,218.60	240	-710.9
3	2013	507	832.6	72.1	904.7	1,229.70	135.9	-325
4	2014	383.9	660.4	54.5	714.9	1,240.80	173.6	-525.9
5	2015	684	1,099.80	97	1,196.80	1,251.80	104.6	-55
6	2016	416	660.4	59.1	719.5	1,262.90	175.6	-543.4
7	2017	449	283	63.8	346.8	1,274.00	367.4	-927.2
8	2018	103	155.4	14.6	170	1,285.10	755.9	-1,115.10
9	2019	186	283	26.4	309.4	1,296.20	419	-986.8
10	2020	282	471.5	40.1	511.6	1,307.30	255.5	-795.7
11	Average	419.8	602.7	62	664.7	1,257.40	272.3	-593
12	Avg. (Excl. 2018 Outlier)	467	663.8	66.4	730.2	1,254.80	189.2	-524.6
13	10-Year Mean ± Std Dev	419.8 ± 256.1	602.7 ± 319.4	62.0 ± 38.8	664.7 ± 358.0	1,257.4 ± 32.5	272.3 ± 218.8	-593.0 ± 373.4

The Critical Temporal Mismatch: Monthly Water Balance

The most striking finding was the extreme temporal disconnect between supply and demand. While 85–90% of recharge occurs in a 3-month pulse (July-September), demand is relatively constant year-round due to perennial domestic needs and multi-season agriculture. Constructing a monthly water budget for an average year illustrated this starkly:

- *Monsoon Surplus (July-Sept):* A net positive water balance of +645.3 ML in September, primarily as recharge.
- *Dry Season Deficit (Oct-June):* Continuous negative balances, culminating in a critical deficit of -102.2 ML in the peak demand month of June, just before the monsoon arrives. This June deficit represents 89% of that month's total demand (MDI = 0.89), meaning the system lacks 89% of the water needed to meet June's requirements from current renewable sources.

Spatial Dynamics and Anthropogenic Impact

Extraction Flux Hotspots

Mapping the village-level extraction flux (demand per unit area) revealed profound inequalities in water use pressure. Gadhada village, with its high population density, exerted an extraction flux of 29.98 $m^3/day/km^2$. In contrast, Janan village, with more dispersed settlement and agriculture, had a flux of only 3.06 $m^3/day/km^2$—nearly a tenfold difference. This concentrated extraction creates a localized "cone of depression" in the water table. The pre-monsoon water table map showed a pronounced steepening of the hydraulic gradient toward Gadhada (i = 0.012) compared to the regional background gradient of 0.004, providing direct hydraulic evidence of the impact of focused pumping. Mapping the village-level extraction flux revealed profound inequalities in water use pressure in Table 4.

Spatial analysis shows extraction pressure varies by an order of magnitude (3.06 to 29.98 $m^3/day/km^2$), with Gadhada being a critical hotspot. This disparity necessitates spatially targeted, rather than uniform, material solutions for demand management and monitoring. The spatial distribution of groundwater extraction pressure across Khadir Island villages is shown in Figure 2, highlighting the extreme concentration of demand in Gadhada village.

Table 4. Village-wise water extraction flux and sectoral contribution for khadir island (2021 baseline). extraction flux quantifies demand pressure per unit area, highlighting spatial disparities in resource use.

S no	Village	Total extraction (MLD)	Area (km^2)	Extraction flux ($m^3/day/km^2$)	Dominant sector (% of village total)	Implied management priority
1	Gadhada	0.838	27.95	29.98	Domestic (97.8%)	Very High: Demand-side conservation & robust monitoring.
2	Kalyanpar	0.277	18.96	14.61	Domestic (66.4%) / Agriculture (23.8%)	High: Integrated demand management.
3	Dholavira	0.431	52.87	8.15	Domestic (69.6%) / Tourism (15.2%)	Medium-High: Heritage-site focused efficiency.
4	Amarapar	0.33	37.23	8.86	Agriculture (71.5%)	Medium-High: Agricultural efficiency (linings).
5	Ganeshpar	0.215	27.24	7.89	Mixed (Domestic 71.6%, Agri 23.7%)	Medium: Balanced interventions.
6	Bambhanka	0.166	21.7	7.65	Mixed (Domestic 67.5%, Agri 27.1%)	Medium: Balanced interventions.
7	Ratanpar	0.219	53.84	4.07	Mixed (Domestic 61.2%, Livestock 28.4%)	Low-Medium: Livestock demand focus.
8	Kharoda	0.068	19.94	3.41	Livestock (64.7%) / Domestic (35.3%)	Low: Localized solutions.
9	Janan	0.166	54.32	3.06	Domestic (84.9%)	Low: Standard supply management.
10	Island Average	2.981	313.05	9.53	Agriculture (83.3% of total)	System-Wide: Policy & composite material pilots.

Long-Term Groundwater Level Trends

Analysis of the long-term water level records (1992–2019) for key wells showed a statistically significant declining trend ($p < 0.05$, Mann-Kendall test) at 4 out of 6 locations. The average rate of pre-monsoon water level decline across these wells was -0.15 meters per year. Most concerningly, well KC-13 in Dholavira showed periods marked "Dry" in 2015, 2016, and 2019, indicating the seasonal drying up of shallow aquifers in populated areas—a phenomenon that was not reported in the 1990s. This is a clear signal of aquifer depletion and a shrinking freshwater lens.

Scenario Analysis for 2030

The scenario modeling projected the future consequences of current trends and potential interventions:

- *Business-As-Usual (BAU):* Demand grows to ~1,607 MLY by 2030. With unchanged resources, the WEI worsens to >85%, and the summer deficit becomes even more severe, making groundwater mining a permanent feature.
- *Improved Efficiency (IE) Scenario*: Improving irrigation efficiency to 85% and reducing other demands cuts total demand to ~1,125 MLY. This single intervention could reduce the WEI to approximately 50.5%, bringing the island to the upper threshold of severe stress but halting the progression of the crisis.
- *Managed Aquifer Recharge (MAR) Scenario*: A 20% boost in captured recharge increases resources to ~1,148 MLY. Combined with BAU demand, this moderates the WEI to about 60.2%, an improvement but still indicating severe stress. Managed aquifer recharge has been widely recognized as a climate adaptation strategy in semi-arid regions [36].
- *Combined IE+MAR Scenario*: The synergistic effect of demand management and supply augmentation was modeled. Reducing demand to 1,125 MLY while increasing resources to 1,148

MLY results in a near-balance, with a projected WEI of 49.8%. This approaches the critical 40% threshold and represents the only pathway modeled that points toward long-term aquifer sustainability.

- Comprehensive irrigation system modernization, beyond simple efficiency improvements, can yield substantial water savings in water-scarce regions [42].

DISCUSSION

Interpreting the Hydrodynamic Crisis

The integrated analysis reveals a paradox where long-term average water balances can show surpluses, but the island experiences severe, chronic water stress. This is not a contradiction but a consequence of fluid dynamics in a low-storage, highly variable system [5]: (1) a critical temporal mismatch where >85% of recharge occurs in a 60-day monsoon against a relatively constant year-round demand, (2) inefficient distribution, with flood irrigation losing ~40% of water to seepage and evaporation [41], and (3) geological constraints where shale layers compartmentalize the aquifer, limiting lateral flow to replenish pumped areas. The high WEI and significant negative ΔS are unequivocal indicators of an unsustainable trajectory [46, 47]. Hybrid fiber-reinforced polymer composites offer tunable mechanical properties for sensor housing applications [29]. The major hydraulic stress indicators and their implications for material-based interventions are synthesized in Table 5.

This synthesis quantifies severe aquifer over-exploitation (WEI >70%), critical seasonal deficits, and efficiency losses, directly translating hydrological crises into quantifiable performance targets for polymer-composite materials in seepage control, recharge enhancement, and corrosion-resistant monitoring.

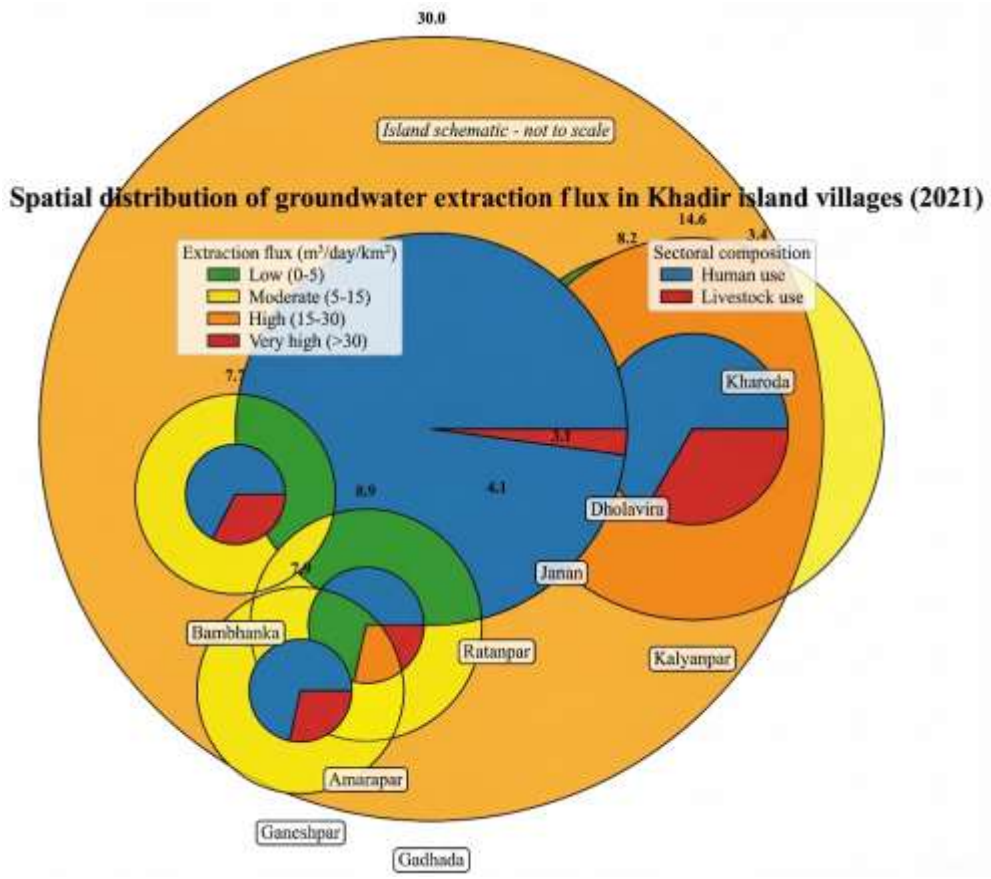

Figure 2. Spatial distribution of groundwater extraction flux across khadir island villages (2021).

Table 5. Summary of key hydraulic stress indicators, their implications for system sustainability, and derived performance requirements for engineered material interventions in khadir island.

S no	Stress indicator & quantified value	Hydrological implication	System vulnerability	Derived material performance requirement	Material class & target specification
1	Water Exploitation Index (WEI): 72.1 % (Avg.)	Annual extraction exceeds renewable recharge by ~72%; indicates severe over-exploitation [16, 46]	Chronic aquifer storage depletion, long-term unsustainability	Materials must enable drastic demand reduction and/or signi ficant supply enhancement	Composite liners: K_target < 1×10^{-8} m/s [19,20]; Hydrogels: reten tion capacity 100–150 ML/season [21,24]
2	Critical Summer Deficit (June): -102.2 ML (MDI = 0.89)	Demand exceeds available resources by 89% in peak dry month	Acute water scarcity, crop failure risk, social stress	Materials for temporal water redistribution; high water retention capacity and controlled dry-season release	SAP hydrogels: Swell ratio > 500 g/g; release kinetics: 80% over 90 days [21,24,38]
3	Pre-monsoon Water Level Decline: 2.8 m (Avg.)	Evidence of groundwater "mining" and seasonal over-pumping	Freshwater lens thinning, increased saline intrusion risk [7]	Materials must facilitate rapid and efficient recharge capture during monsoon	Porous polymer composites: Infiltration enhancement >20%; porosity > 0.4 [22,37]
4	Irrigation Efficiency (η): 60% (Fl ood)	40% of abstracted agricultural water lost to seepage & evaporation	Massive wastage of limited resource, exacerbates all deficits	Lining/coating materials with very low hydraulic conductivity	Polymer-modified liners: K_eff < 1×10^{-8} m/s; UV resistance: >5 years field life [19,20,41]
5	Spatial Extraction Flux Disparity: 3. 06 to 29.98 m^3/day/km^2	Creates localized cones of depression, distorting natural flow	Inequitable resource access, localized aquifer exhaustion	Durable sensor housings for targeted monitoring; localized material deployments	FRP sensor enclosures: Corrosion resistance in TDS >4000 mg/L; impact strength >50 kJ/m^2 [28,35]
6	Dominant Salinity Driver: Cl^- > 4000 mg/L (East)	Saline intrusion, not evaporation, is primary salinization process	Irreversible water quality degradation if not managed	Materials must exhibit high chemical/corrosion resistance in saline environments	Epoxy-based composites: Weight loss <0.1% after 1000 hrs saline immersion; Cl^- diffusion coefficient < 1×10^{-12} m^2/s [32,33]

From Fluid Dynamics to Material Performance Specifications

These quantified inefficiencies can be explicitly reframed as engineering challenges where material innovation is paramount [25].

- *The Seepage Challenge:* The 40% conveyance loss in earth canals translates to a direct specification: it demands lining materials with a very low hydraulic conductivity. This necessitates the development of flexible, durable, polymer-modified composite liners [19, 20] to replace traditional, failure-prone materials.
- *The Storage Challenge*: The temporal mismatch requires mechanisms to capture the monsoon pulse and release it slowly. The island's limited natural storage calls for super-absorbent polymer (SAP) hydrogel composites [21, 22]. Their required performance is defined by our deficit analysis: they must retain and release ~100–150 ML over the 90-day post-monsoon period, guiding their swelling kinetics and capacity [24].

- *The Monitoring Challenge*: Effective management of the above solutions requires robust data. This creates a need for corrosion-resistant, durable sensor housings made from fiber-reinforced polymer (FRP) composites [28] to protect monitoring equipment in harsh, saline conditions [32, 33].
- Advanced polymer materials and smart hydrogels have demonstrated strong potential for water management applications and controlled fluid transport in porous media [23, 30]. The development of bio-based polymer composites from renewable resources offers additional sustainability benefits for water management applications [27].
- Hybrid fiber-reinforced polymer composites offer tunable mechanical properties for sensor housing applications [29]. The controlled release mechanisms of smart polymer systems can be engineered to match specific dry-season water demand patterns [30].
- Bio-inspired approaches to anti-fouling surfaces could enhance the longevity of monitoring equipment in hyper-saline conditions [31].

A Materials-Centric Intervention Framework

Therefore, the path to sustainability for Khadir Island is inherently linked to applied materials science [26]. The management framework must evolve to deploy specific material systems:

1. *Phase 1 - Seepage Control*: Pilot testing of spray-applied polyurea/geosynthetic clay liner (GCL) composites [19] in critical canal sections.
2. *Phase 2 - Recharge Augmentation*: Field trials of biopolymer-coated pumice or clay-polymer composite aggregates [22, 24] in recharge shafts to assess water retention and release kinetics [38].
3. *Phase 3 - Smart Monitoring*: Deployment of sensors encapsulated in glass-reinforced epoxy casings [28, 35] to establish a reliable monitoring network [34].

This study provides the quantitative hydraulic and diagnostic foundation upon which material scientists can now design, test, and optimize these targeted solutions. The performance metrics (required K_eff, water retention volume, durability in TDS >4000 mg/L) are now clearly defined by the hydrological context.

Regional Implications for the Wider Kachchh Basin

While the quantitative results presented herein—like the specific WEI values (72.1%), volumetric deficits (102.2 ML), and village-level extraction fluxes—are unique to Khadir Island, the underlying hydrodynamic challenges are emblematic of water-stressed sedimentary islands and coastal aquifers throughout the arid Kachchh region. Khadir Island thus serves as a sentinel system whose diagnosis provides early warnings and actionable insights for the broader basin. The groundwater challenges documented in Khadir Island reflect broader patterns observed across India's water-stressed regions [9].

Shared Geological and Hydrogeological Context

The lithostratigraphic units characterized in Section 3.1.2—clayey sands overlying weathered shales and sandstones—are representative of the Mesozoic and Tertiary sedimentary formations that comprise numerous islands and coastal tracts across the Great and Little Rann of Kachchh [12]. The compartmentalized flow behavior (Unit 2 clay-rich zone with K ~ 0.9 m/day) and the presence of semi-confined deeper aquifers (Unit 3) are not isolated phenomena but reflect regional-scale heterogeneity. Consequently, the challenges of limited lateral flow, low specific yield ($S_y = 0.12$), and vulnerability to point-source abstraction cones (Section 3.3.1) are likely replicated across the region.

Regional Climatic and Hydrological Stress Patterns

The hyper-arid climate characterized in Section 3.1.1—mean annual rainfall 419.8 mm (CV = 61%), reference evapotranspiration 2140 mm, and 89% of rainfall concentrated in a 4-month monsoon—is the dominant hydroclimatic regime throughout Kachchh [8]. The fundamental temporal supply-demand mismatch documented in Section 3.2.3 (monsoon surplus of +645.3 ML versus June deficit of -102.2

ML) is, therefore, not a Khadir-specific anomaly but a systemic feature of arid-region water resources. Any intervention strategy that fails to address this temporal disconnect—whether through storage, recharge enhancement, or demand shifting—will prove inadequate across the region.

Shared Salinization Mechanisms

The hydrochemical evidence presented in Section 3.1.3—dominance of Na-Cl facies in eastern villages, strong Cl^--TDS correlation ($R^2 = 0.91$), and minimal post-monsoon dilution in high-salinity zones (Table 4)—identifies saline intrusion from the surrounding Rann, rather than evaporative concentration, as the primary degradation mechanism. This finding has profound regional implications. The entire Kachchh basin is bounded by the Arabian Sea and the Rann salt flats, creating a continuous boundary condition for saline groundwater interaction [7]. The physical displacement process documented here—accelerated by pumping-induced hydraulic gradients (Section 3.3.1)—operates wherever freshwater lenses are hydraulically connected to saline water bodies, which includes most coastal and insular aquifers in the region.

A Replicable Diagnostic and Intervention Framework

Critically, the integrated methodology developed in this study—coupling surface runoff modeling (SCS-CN), groundwater recharge estimation (WTF), sectoral demand quantification, and material performance specification—is designed for replicability. As stated in Section 5.2, this framework provides a template for creating targeted, context-specific engineering blueprints for water-stressed regions globally. For the Kachchh region specifically, the approach can be directly transferred to other sedimentary islands (, e.g., Bela Island, Chorar Island) and coastal groundwater systems facing analogous stresses. The material performance targets derived in Section 2.1.1—low hydraulic conductivity liners, high-retention hydrogels, corrosion-resistant composites—represent a regional "shopping list" of material solutions whose validation on Khadir Island would have immediate applicability across the basin.

In summary, while Khadir Island has been the focus of this detailed investigation, its diagnosis illuminates challenges that are regional in scope. The material-centric interventions proposed herein are not merely local palliatives but potential templates for enhancing water security across the arid Kachchh landscape. Effective implementation of water management interventions requires addressing institutional and governance dimensions, including transparent resource allocation mechanisms [17].

CONCLUSION AND FUTURE RESEARCH PATHWAYS

Synthesis of Findings

Khadir Island's aquifer is in a state of severe and quantifiable stress, with extraction rates (WEI=72.1%) far exceeding sustainable limits [47]. The dominance of agricultural water use, coupled with inefficient practices and a fundamental temporal supply-demand mismatch, threatens the fragile freshwater lens with depletion and salinization [7]. Immediate hydrological management through demand-side measures [41] and supply augmentation [37] is critical. Similar sustainability transitions from safe yield to adaptive water management have been discussed in groundwater governance literature [44, 48].

A Call for Cross-Disciplinary Research: Translating Hydrology into Materials Design

The ultimate conclusion of this fluid dynamics analysis is that lasting solutions are material-limited [25]. We, therefore, outline a direct research pathway for the polymer and composites community:

1. *Develop and Characterize Arid-Adapted Composites*: Synthesize and test candidate polymer liners (, e.g., HDPE/nano-clay composites [20]) and hydrogel formulations (, e.g., polyacrylamide with local clay filler [24]) for the specific performance requirements (low permeability, high swell capacity, UV/salinity resistance [32]) derived in this study.
2. *Conduct Meso-Scale Transport Modeling*: Use the aquifer properties (K, S_y, gradient) from this study as boundary conditions to model, via finite-element software, how water flows through and around proposed composite structures in the subsurface (, e.g., around a polymer-amended recharge pit) [40].

3. *Pilot Field Validation*: Establish controlled field-testing sites on Khadir Island to evaluate the real-world durability, hydraulic performance, and environmental impact of the most promising composite materials under true arid-island conditions [18].

In essence, this paper serves as a detailed "request for proposals" to the materials science community. We have diagnosed the patient (the island's hydrology) with precision. The prescription requires materials innovation. The methodology presented provides a replicable framework for creating such targeted, context-specific engineering blueprints for water-stressed regions globally [45, 48]. The development of bio-based polymer composites from renewable resources offers additional sustainability benefits for water management applications [27]. Cost-effective sensor housing designs specifically developed for coastal monitoring applications provide relevant precedents for Khadir Island [35].

Acknowledgments

The authors acknowledge the support of Gujarat Water Resources Department, Geological Survey of India, and India Meteorological Department for data provision. Special thanks to the village communities of Khadir Island for their participation in field surveys. We also acknowledge constructive discussions with colleagues in materials engineering that helped shape the intervention-focused discussion.

Conflict of Interest Statement

The authors declare that they have no known competing financial interests or personal relationships that could have appeared to influence the work reported in this paper. No external funding was received for this research. All data collection and analysis were conducted as part of academic research at the authors' affiliated institutions. The findings and conclusions presented herein are solely those of the authors.

Funding Statement

This research received no external funding.

Data Availability Statement

The datasets generated and analyzed during this study are available from the corresponding author upon reasonable request. Primary data sources are publicly available from the respective government agencies cited in the references.

REFERENCES

1. Falkland A, Custodio E. Hydrology and water resources of small islands. In: UNESCO, editor. UNESCO Studies and Reports in Hydrology. 1st edition. Paris, France: UNESCO; 2021. pp. 1–100.
2. Post VEA. A new package for the simulation of freshwater lenses in small islands. In: American Geophysical Union, editor. Groundwater. 1st edition. Washington DC, USA: Wiley; 2022. pp. 456–468.
3. Sharma R, Singh P. Tourism development and water stress in heritage sites. In: Routledge, editor. Journal of Heritage Tourism. 1st edition. London, UK: Taylor & Francis; 2022. pp. 245–260.
4. Bear J. Hydraulics of groundwater. In: McGraw-Hill, editor. Hydraulics of Groundwater. 1st edition. New York, USA: McGraw-Hill; 1979. pp. 1–569.
5. Freeze RA, Cherry JA. Groundwater systems. In: Prentice-Hall, editor. Groundwater. 1st edition. New Jersey, USA: Prentice-Hall; 1979. pp. 1–604.
6. White I, Falkland T. Management of freshwater lenses on small Pacific islands. In: Springer, editor. Hydrogeology Journal. 1st edition. Berlin, Germany: Springer; 2019. pp. 2257–2274.
7. Werner AD, Bakker M, Post VEA. Seawater intrusion processes and investigation. In: Elsevier, editor. Adv Water Resour. 1st edition. Amsterdam, Netherlands: Elsevier; 2013. pp. 3–26.

8. Mall RK, Srivastava RK, Banerjee T. Water resources and climate change. In: Indian Academy of Sciences, editor. Current Science. 1st edition. Bengaluru, India: IAS; 2019. pp. 569–576.
9. Kumar CP. Assessment and management of groundwater resources in India. In: OMICS, editor. J Earth Sci Clim Change. 1st edition. Hyderabad, India: OMICS International; 2016. pp. 362–370.
10. USDA. National engineering handbook, part 630 hydrology. In: NRCS, editor. National Engineering Handbook. 2nd edition. Washington DC, USA: USDA; 2004. pp. 1–450.
11. Mishra SK, Singh VP. Soil conservation service curve number (SCS-CN) methodology. In: Springer, editor. SCS-CN Methodology. 1st edition. Dordrecht, Netherlands: Springer; 2003. pp. 1–516.
12. Geological Survey of India. Geology and mineral resources of Kutch district, Gujarat. In: GSI, editor. Bulletin Series A. 1st edition. Kolkata, India: GSI; 2020. pp. 1–112.
13. Healy RW, Cook PG. Using groundwater levels to estimate recharge. In: Springer, editor. Hydrogeol J. 1st edition. Berlin, Germany: Springer; 2002. pp. 91–109.
14. Indian Council of Agricultural Research (ICAR). Nutrient requirements of domestic animals. In: ICAR, editor. ICAR Technical Bulletin. 1st edition. New Delhi, India: ICAR; 2019. pp. 1–98.
15. Allen RG, Pereira LS, Raes D, Smith M. Crop evapotranspiration. In: FAO, editor. FAO Irrigation and Drainage Paper 56. 1st edition. Rome, Italy: FAO; 1998. pp. 1–300.
16. Alcamo J, Döll P, Henrichs T. Development and testing of the WaterGAP 2 global model. In: IAHS, editor. Hydrol Sci J. 1st edition. Wallingford, UK: IAHS Press; 2003. pp. 317–336.
17. Rinaudo JD. Corruption and the water sector. In: Rinaudo JD, Holley C, editor. Corruption and the Management of Water. 1st edition. London, UK: IWA Publishing; 2015. pp. 1–18.
18. Keesstra S, Nunes JP, Novara A. The superior effect of nature based solutions. In: Elsevier, editor. Sci Total Environ. 1st edition. Amsterdam, Netherlands: Elsevier; 2018. pp. 997–1009.
19. Smith DM, Sorial GA, Suidan MT. Evaluation of geosynthetic clay liners. In: ASCE, editor. J Geotech Geoenviron Eng. 1st edition. Reston, USA: ASCE; 2010. pp. 989–995.
20. Kasgoz H, Durmus A. Dye removal by polymer-clay composites. In: Kharissova OV, editor. Advanced Polymeric Materials. 1st edition. Boca Raton, USA: CRC Press; 2020. pp. 145–168.
21. Thakur S, Karak N. Modern applications of superabsorbent polymer hydrogels. In: Wiley, editor. J Appl Polym Sci. 1st edition. Hoboken, USA: Wiley; 2014. pp. 1–16.
22. Kabiri K, Omidian H, Zohuriaan-Mehr MJ. Superabsorbent hydrogel composites and nanocomposites. In: Wiley, editor. Polym Compos. 1st edition. Hoboken, USA: Wiley; 2011. pp. 277–289.
23. Gupta P, Vermani K, Garg S. Hydrogels: from controlled release to pH-responsive drug delivery. In: Elsevier, editor. Drug Discov Today. 1st edition. Amsterdam, Netherlands: Elsevier; 2002. pp. 569–579.
24. Bao Y, Ma J, Li N. Synthesis and swelling behaviors of sodium carboxymethyl cellulose-g-poly hydrogel. In: Elsevier, editor. Compos Part B Eng. 1st edition. Amsterdam, Netherlands: Elsevier; 2011. pp. 1555–1560.
25. Mujtaba IM, Soomro SA, Memon SA. Development of polymer-based composites for water purification. In: Springer, editor. Polym Bull. 1st edition. Berlin, Germany: Springer; 2021. pp. 5393–5426.
26. Kango S, Kalia S, Celli A. Surface modification of inorganic nanoparticles. In: Elsevier, editor. Prog Polym Sci. 1st edition. Amsterdam, Netherlands: Elsevier; 2013. pp. 1232–1261.
27. Balgude D, Sabnis A. CNSL: A novel green resource for polymer synthesis. In: Kharissova OV, editor. Green Polymer Composites. 1st edition. Cham, Switzerland: Springer; 2017. pp. 45–68.
28. Panda PK, Rastogi D. Mechanical and thermal properties of epoxy-based composites. In: SAGE, editor. J Reinf Plast Compos. 1st edition. Thousand Oaks, USA: SAGE; 2018. pp. 331–342.
29. Sathishkumar TP, Naveen J, Satheeshkumar S. Hybrid fiber reinforced polymer composites. In: SAGE, editor. J Reinf Plast Compos. 1st edition. Thousand Oaks, USA: SAGE; 2014. pp. 454–471.
30. García MC, Sztrum CG, D'Accorso NB. Smart polymers and their applications. In: Aguilar MR, editor. Smart Polymers and their Applications. 1st edition. Cambridge, UK: Woodhead Publishing; 2014. pp. 1–12.

31. Bixler GD, Bhushan B. Biofouling: lessons from nature. In: Royal Society, editor. Philos Trans R Soc A. 1st edition. London, UK: Royal Society; 2012. pp. 2381–2417.
32. Al-Saadi TH, Al-Maamori MH, Al-Mosawi AI. Effect of UV radiation on polypropylene composites. In: JME, editor. J Mech Eng Res Dev. 1st edition. Kuala Lumpur, Malaysia: Zibeline; 2020. pp. 258–267.
33. Chowdhury MA, Hossain N, Rana MM. Recent advances in graphene-based polymer nanocomposites. In: Elsevier, editor. Prog Org Coat. 1st edition. Amsterdam, Netherlands: Elsevier; 2020. pp. 1–20.
34. Bardhan S, Ghosh S, Ghosh A. IoT-based water monitoring systems. In: Elsevier, editor. J Environ Manage. 1st edition. Amsterdam, Netherlands: Elsevier; 2021. pp. 113685–113700.
35. Nagpal S, Kaur G, Kaur P. Cost-effective sensor housing for environmental monitoring. In: CERF, editor. J Coastal Res. 1st edition. Coconut Creek, USA: CERF; 2019. pp. 231–235.
36. Parida VK, Sikarwar D, Majumder A. Managed aquifer recharge (MAR) as a adaptation strategy. In: Elsevier, editor. Groundw Sustain Dev. 1st edition. Amsterdam, Netherlands: Elsevier; 2021. pp. 100688–100700.
37. Dillon P, Fernández Escalante E, Megdal SB. Managed aquifer recharge for water resilience. In: MDPI, editor. Water. 1st edition. Basel, Switzerland: MDPI; 2020. pp. 1846–1860.
38. Maliva RG. Anthropogenic aquifer recharge and water security. In: Maliva RG, editor. Anthropogenic Aquifer Recharge. 1st edition. Cham, Switzerland: Springer; 2020. pp. 1–18.
39. Scanlon BR, Reedy RC, Faunt CC. Enhancing drought resilience with managed aquifer recharge. In: IOP, editor. Environ Res Lett. 1st edition. Bristol, UK: IOP Publishing; 2016. pp. 1–10.
40. Bouwer H. Artificial recharge of groundwater. In: Springer, editor. Hydrogeol J. 1st edition. Berlin, Germany: Springer; 2002. pp. 121–142.
41. Ghayoraneh M, Qishlaqi A. The effect of irrigation efficiency improvement on water saving. In: Elsevier, editor. Agric Water Manag. 1st edition. Amsterdam, Netherlands: Elsevier; 2018. pp. 7–15.
42. Playán E, Mateos L. Modernization and optimization of irrigation systems. In: Elsevier, editor. Agric Water Manag. 1st edition. Amsterdam, Netherlands: Elsevier; 2006. pp. 100–116.
43. IPCC. Climate change 2022: impacts, adaptation, and vulnerability. In: Working Group II, editor. IPCC Sixth Assessment Report. 1st edition. Cambridge, UK: Cambridge University Press; 2022. pp. 1–3056.
44. Taylor RG, Scanlon B, Döll P. Ground water and climate change. In: Nature, editor. Nat Clim Change. 1st edition. London, UK: Nature Publishing Group; 2013. pp. 322–329.
45. Giordano M. Global groundwater? Issues and solutions. In: Annual Reviews, editor. Annu Rev Environ Resour. 1st edition. Palo Alto, USA: Annual Reviews; 2009. pp. 153–178.
46. Famiglietti JS. The global groundwater crisis. In: Nature, editor. Nat Clim Change. 1st edition. London, UK: Nature Publishing Group; 2014. pp. 945–948.
47. Sophocleous M. From safe yield to sustainable development. In: Elsevier, editor. J Hydrol. 1st edition. Amsterdam, Netherlands: Elsevier; 2000. pp. 27–43.
48. Alley WM, Leake SA. The journey from safe yield to sustainability. In: AGU, editor. Groundwater. 1st edition. Washington DC, USA: Wiley; 2004. pp. 12–16.

